



PUBLISHED BY INSTITUTE OF PHYSICS PUBLISHING FOR SISSA/ISAS

RECEIVED: December 3, 2002

ACCEPTED: January 10, 2003

Perturbative computation of glueball superpotentials for $SO(N)$ and $USp(N)$

Harald Ita,^a Harald Nieder^a and Yaron Oz^{ab}

^a*Raymond and Beverly Sackler Faculty of Exact Sciences
School of Physics and Astronomy
Tel-Aviv University, Ramat-Aviv 69978, Israel*

^b*Theory Division, CERN*

CH-1211 Geneva 23, Switzerland

*E-mail: ita@post.tau.ac.il, harald@post.tau.ac.il, yaranoz@post.tau.ac.il,
Yaron.Oz@cern.ch*

ABSTRACT: We use the superspace method of [18] to prove the matrix model conjecture for $\mathcal{N} = 1$ $USp(N)$ and $SO(N)$ gauge theories in four dimensions. We derive the prescription to relate the matrix model to the field theory computations. We perform an explicit calculation of glueball superpotentials. The result is consistent with field theory expectations.

KEYWORDS: Nonperturbative Effects, Supersymmetric Effective Theories, Matrix Models.

JHEP01(2003)018

Contents

1. Introduction	1
2. Review of superspace	2
3. The perturbative computation	4
4. Reduction to S^2 and RP^2 graphs	5
4.1 Why S^2 and RP^2 graphs	5
4.2 Perturbative superpotential	6
5. Proof of matrix model conjecture	7
5.1 The interior graph	7
5.2 The exterior graph	8
6. Discussion of matrix model conjectures	9
7. Perturbative superpotential computations	10
7.1 General prescription	10
7.2 Explicit calculations	11
7.3 Discussion of example	11
A. Double line notation	12
A.1 Double line notation for $SO(N)$	12
A.2 Double line notation for $USp(N)$	13
B. The matrices L_{ia}, K_{im}	14
B.1 Planar diagrams	14
B.2 Non-oriented diagrams	15
B.2.1 The first non-oriented diagram	15
B.2.2 The second non-oriented diagram	16

1. Introduction

In a recent series of seminal papers [1]–[3] Dijkgraaf and Vafa proposed a matrix model approach for calculating holomorphic quantities in $\mathcal{N} = 1$ supersymmetric field theories in four dimensions. Their proposal has been tested in a variety of contexts [4]–[8] and extended to theories with flavors [9]–[12]. These techniques have been also applied to four-dimensional $\mathcal{N} = 2$ supersymmetric gauge theories [13]. Other interesting features of

this approach have been discussed in [14, 15] and an analysis beyond the planar limit has been performed in [16]. In [17] the Konishi anomaly was used to elucidate the connection of the effective superpotential to the matrix model.

A field theoretic proof of the conjecture of Dijkgraaf and Vafa was given in [18]. In this paper it has been shown that superspace techniques can be used to compute the perturbative part of the glueball super-potential in $U(N)$ $\mathcal{N} = 1$ gauge theories with one adjoint chiral superfield. The gauge sector was treated as background. As noted already by Dijkgraaf et al the line of argument should apply equally well to the gauge groups $USp(N)$ and $SO(N)$. The aim of this paper is to extend the known methods and verify the claim.

We consider one adjoint chiral superfield in an external gauge field with $\mathcal{N} = 1$ supersymmetry. We wish to calculate the effective superpotential of the glueball superfield after integrating over the chiral superfield. The calculation has to be done by summing Feynman diagrams for the dynamical field. The Feynman diagrams can be organized in an expansion in terms of a small glueball superfield. We prove that as in the case of a $U(N)$ gauge group the computation of the Feynman graphs simplifies to graphs of a zero dimensional field theory, as proposed in [3].

However, the precise prescription to relate the matrix model partition function to the effective super-potential has to be adapted. Applying our results, we will calculate the perturbative superpotential up to order three in the glueball field for a quartic tree level superpotential. We will find a numerical disagreement with the original conjecture.

The paper is organized in seven sections. In section 2 we define the theory and the observable we want to study. We then summarize briefly the superspace calculations of [18]. In section 3 we review the convenient language for the perturbative calculations. In section 4 we argue that only Feynman graphs (in double line notation) on S^2 and RP^2 contribute to the perturbative calculations. In section 5 we prove that the field theory calculation can be reduced to a matrix model computation. The explicit prescription to relate field theory and matrix model computations is then discussed in section 6. The final section 7 contains an example computation as well as a discussion of the result. In the appendix we have included details about the double line notation for $SO(N)$ and $USp(N)$ and sample calculations with methods to calculate Feynman graphs with insertions developed and used in section 4 and 5.

2. Review of superspace

We start with a short review of the superspace calculation performed in [18]. This calculation does not depend on the gauge group and we will therefore restrict ourselves to those aspects which are most important for our subsequent analysis.

The starting point is the following four dimensional action for a massive chiral superfield Φ coupled to an external gauge field with the self interaction determined by the gauge invariant super-potential $W(\Phi)$

$$S(\Phi, \bar{\Phi}) = \int d^4x d^4\theta \bar{\Phi} e^V \Phi + \int d^4x d^2\theta W(\Phi) + \text{h.c.}, \quad (2.1)$$

where, following the conventions given in [19], the gauge field strength is given by

$$\mathcal{W}_\alpha = i\bar{D}^2 e^{-V} D_\alpha e^V. \quad (2.2)$$

We are looking for the perturbative part¹ of the effective superpotential of this system

$$\int d^2\theta W_{\text{eff}}^{\text{pert.}}(S) \quad (2.3)$$

as a function of the (traceless) external glueball superfield $S \sim \mathcal{W}_\alpha \mathcal{W}^\alpha$. The full effective superpotential also includes the Veneziano-Yankielowicz term [22]. As we will see $W_{\text{eff}}^{\text{pert.}}$ can be calculated from summing a certain subset of Feynman graphs.

For the perturbative analysis we should take into account the holomorphic propagator $\langle \Phi \Phi \rangle$ as well as the anti-holomorphic propagator $\langle \bar{\Phi} \bar{\Phi} \rangle$ and the mixed propagator $\langle \Phi \bar{\Phi} \rangle$. However, as argued in [18], by holomorphy arguments we are led to the conclusion that the superpotential for a chiral glueball superfield cannot depend on the coefficients of the anti-chiral superpotential and thus only holomorphic propagators contribute.

This was put to use in [18] by choosing the following simple quadratic form for the anti-chiral superpotential

$$\bar{W}(\bar{\Phi}) = \frac{1}{2} \bar{m} \bar{\Phi}^2. \quad (2.4)$$

This choice allows to integrate out the anti-chiral superfield $\bar{\Phi}$. Furthermore by taking into account that we are looking for the effective potential of a constant glueball superfield $S \sim \mathcal{W}^\alpha \mathcal{W}_\alpha$ it is shown in [18] that one ends up with the action

$$S = \int d^4x d^2\theta \left(-\frac{1}{2\bar{m}} \Phi (\square - i\mathcal{W}^\alpha D_\alpha) \Phi + W_{\text{tree}}(\Phi) \right), \quad (2.5)$$

where \bar{m} is the mass term that appeared in the anti-chiral superpotential (2.4). The chiral tree-level superpotential will take the form

$$W_{\text{tree}}(\Phi) = \frac{m}{2} \Phi^2 + \text{interactions}. \quad (2.6)$$

As was mentioned above and as is shown explicitly in [18] the path integral does not depend on \bar{m} and we will set $\bar{m} = 1$. This turns out to be the most convenient value for \bar{m} if we want to follow the approach of [18] and evaluate the partition function perturbatively. This leads to

$$\frac{1}{p^2 + m + \mathcal{W}^\alpha \pi_\alpha} \quad (2.7)$$

for the momentum space propagator. Note that after Fourier transforming the fermionic superspace directions the derivative D_α is given by the fermionic momentum π_α

$$D_\alpha = -i\pi_\alpha. \quad (2.8)$$

¹Here perturbative means perturbative in the field S , as is common in the literature on this subject.

3. The perturbative computation

As was shown for planar diagrams in [18], Feynman amplitudes for the observable (2.3) in the field theory (2.1) with gauge group $U(N)$ and Φ in the adjoint representation simplify drastically, when written in terms of Schwinger parameters. Actually, the simplification allows to reduce calculations to that of matrix models. Similar reasoning will be possible for the gauge groups $SO(N)$ and $USp(N)$. In this section we will introduce the Schwinger parameterization, perform integrations over bosonic loop momenta and point out the peculiarities of the fermionic momentum integration.

Given a Feynman graph, we can write its propagators (2.7) as integrals over Schwinger parameters s_i , where the index i runs over the edges of the Feynman diagram,

$$\int_0^\infty ds_i \exp \left[-s_i(p_i^2 + \mathcal{W}_i^\alpha \pi_{i\alpha} + m) \right]. \quad (3.1)$$

Now the momentum integrals are gaussian integrals and can be evaluated. To this end we express the momenta p_i , that flow through the i -th propagator in terms of loop momenta k_a ²

$$p_i = \sum_a L_{ia} k_a. \quad (3.2)$$

With the conventions

$$M_{ab}(s) = \sum_i s_i L_{ia} L_{ib} \quad (3.3)$$

the integral over the bosonic momenta in all loops can be performed

$$Z_{\text{boson}} = \int \prod_{a=1}^l \frac{d^4 k_a}{(2\pi)^4} \exp \left[- \sum_{a,b} k_a M_{ab}(s) k_b \right] = \frac{1}{(4\pi)^{2l}} \frac{1}{(\det M(s))^2}. \quad (3.4)$$

It will turn out later, that the factor $(\det M(s))^{-2}$ gets canceled by the integral over the fermionic momenta π .

Also, we integrate over the fermionic loop momenta. With the relation

$$\pi_{i\alpha} = \sum_a L_{ia} \kappa_{a\alpha} \quad (3.5)$$

between the fermionic momentum $\pi_{i\alpha}$ running through the i -th propagator and the fermionic loop momentum $\kappa_{a\alpha}$, the fermionic integral takes the form

$$\int \prod_a d^2 \kappa_a \exp \left[- \sum_i s_i \left(\sum_a \mathcal{W}_i^\alpha L_{ia} \kappa_{a\alpha} \right) \right]. \quad (3.6)$$

The fields $\mathcal{W}_{i\alpha} = \sum_A \mathcal{W}_A^\alpha T_{Rep(i)}^A$ are matrix-valued and are inserted on the i -th edge of the Feynman diagram in the representation $Rep(i)$ of the field propagating through this edge. From now on we will consider one propagating field transforming in the adjoint representation.

²Throughout this letter we will use the following conventions for indices: indices i, j, \dots denote the various propagators, indices a, b, \dots denote loops and the indices m, n, \dots denote index loops.

4. Reduction to S^2 and RP^2 graphs

In this section we will review why only the graphs on S^2 and RP^2 contribute to the effective superpotential. We will give the explicit form of the Feynman amplitudes that contribute to the superpotential for $SO(N)$ and $USp(N)$.

4.1 Why S^2 and RP^2 graphs

To understand why only S^2 and RP^2 graphs contribute we have to consider the \mathcal{W}^α insertions and the fermionic integrals (3.6) in more detail.

The 't Hooft double line notation helps to handle the insertions \mathcal{W}^α for the $SO(N)$ and $USp(N)$ gauge groups. However, for these groups the propagators are represented not only by parallel lines, but also by crossed lines. As a consequence of the crossed lines 't Hooft diagrams can be associated to orientable and non orientable Riemann surfaces.

The 't Hooft diagrams at l loops have at most $h = l + 1$ holes (including the outer boundary for planar diagrams). The diagrams with l loops that do not have less than l holes are the planar ones and the non orientable ones, that can be drawn on RP^2 . We will see shortly why these are the only relevant diagrams for our calculation.

We want to calculate the effective potential for the traceless glueball superfield S . The perturbative expansion of the potential includes graphs with multiple insertions of \mathcal{W} on the index loops. For example, inserting \mathcal{W} a_m times on the index loop m will give an overall factor

$$\prod_m \text{Tr}(\mathcal{W}^{a_m}), \quad (4.1)$$

for a given Feynman diagram. However, as we are interested in the chiral observable (2.3), we choose the background field \mathcal{W}^α such that the higher traces $\text{Tr}(\mathcal{W}^n)$ vanish for $n > 2$.

The integration over the fermionic loop momenta brings down a factor of \mathcal{W}^2 for each loop. As follows from above, these have to be distributed in pairs to the index loops. This requires that the number of index loops be greater than or equal to the number of momentum loops.

The only oriented diagrams that meet this requirement are the planar ones, which have $l+1$ index loops. The only non-vanishing oriented diagrams are thus the planar ones with two insertions of \mathcal{W} on each but one index loop.

Considering the non-oriented diagrams for the groups $SO(N)$ and $USp(N)$ it is found that diagrams that can be drawn on RP^2 are singled out by the above requirement. Such diagrams with l loops have l index loops. Consequently, the non-vanishing non-oriented diagrams have exactly two insertions of \mathcal{W} on each index loop.

A convenient way to implement the requirement of having two insertions for each index loop is to introduce auxiliary fermionic variables similar to what was done in [18]. However, we will assign our auxiliary variables to the index loops and not to the loops. A detailed description of how the appropriate transformation matrices are obtained is given in appendix B.

Hence, we expand the background field \mathcal{W}_i^α as

$$\mathcal{W}_i^\alpha = K_{im} \mathcal{W}_m^\alpha. \quad (4.2)$$

Collecting the contributions of the \mathcal{W}^α insertions for a diagram γ one finds the general formula

$$\begin{aligned} Z_{\text{ferm.}}^\gamma &:= \int \prod_{a,m} d^2\kappa_a d^2\mathcal{W}_m \exp \left[- \sum_i s_i \left(\sum_{m,a} \mathcal{W}_m^\alpha K_{mi}^T L_{ia} \kappa_{a\alpha} \right) \right] \\ &= \det(N(s))^2, \end{aligned} \quad (4.3)$$

where we write the s -dependence of the above integrands in a concise way as

$$N(s)_{ma} = \sum_i s_i K_{mi}^T L_{ia}. \quad (4.4)$$

The s -dependence of the Feynman amplitude is then given by

$$Z = Z_{\text{boson}} Z_{\text{ferm.}} = \frac{1}{(4\pi)^{2l}} \left(\frac{\det(N(s))}{\det(M(s))} \right)^2. \quad (4.5)$$

4.2 Perturbative superpotential

Before we turn to the evaluation of Z we pause for a while to write the Feynman amplitudes in terms of the notation we have developed so far.

We use the definition for the glueball superfield

$$S = \frac{1}{32\pi^2} \text{Tr}[\mathcal{W}^\alpha \mathcal{W}_\alpha], \quad (4.6)$$

to express the amplitudes in terms of S . The amplitude corresponding to a planar diagram γ can then be written as

$$A_{\text{planar}}^\gamma = N h c_\gamma (16\pi^2 S)^{h-1} \int \prod_i ds_i e^{-s_i m} Z(\gamma, s). \quad (4.7)$$

N comes from the summation over the free index loop. This factor is the same as for $U(N)$. The factor h is combinatorial and counts the number of ways to pick one free index loop out of a total of h . Finally, c_γ denotes the multiplicity of the graph γ .

For a diagram γ on RP^2 we have

$$B_{RP^2}^\gamma = \sigma c_\gamma (16\pi^2 S)^h \int \prod_i ds_i e^{-s_i m} Z(\gamma, s). \quad (4.8)$$

This general amplitude exhibits some important differences compared to the planar amplitude (4.7). First, we do not have any index loop without insertions. Therefore, the factor N , that we have in the planar case is absent. Secondly, the factor σ , which takes the values ± 1 , serves to distinguish the group $SO(N)$ from $USp(N)$. This is due to the fact that the propagator for the adjoint of $USp(N)$ also includes the skew-symmetric $USp(N)$ invariant J whose insertions give an overall minus sign for the $USp(N)$ as compared to $SO(N)$ for the RP^2 diagrams. The details are given in appendix A.

In terms of these amplitudes the perturbative part of the effective superpotential is given as a function of S as

$$W_{\text{eff}}^{\text{pert.}}(S) = \sum_\gamma \left(A_{\text{planar}}^\gamma + B_{RP^2}^\gamma \right). \quad (4.9)$$

The amplitudes can be generated from a zero-dimensional field theory if $Z(\gamma, s)$ is independent of s . This has been shown for $U(N)$ gauge group in [18]. Similarly the s -dependence vanishes for $SO(N)$ and $USp(N)$, as we will show in the next section.

5. Proof of matrix model conjecture

In this section we calculate the value of the ratio λ of the fermionic to the bosonic determinant,

$$\lambda = \left(\frac{\det(N(s))}{\det(M(s))} \right)^2. \quad (5.1)$$

We will show that the ratio λ does not depend on the Schwinger parameters s_i and we will calculate its value explicitly for an arbitrary Feynman graph on S^2 as well as on RP^2 . We find that $\lambda = 1$ on S^2 and $\lambda = 4$ on RP^2 .

For the following it will be convenient to think of RP^2 as a disk with opposite points on the boundary identified.

In order to actually calculate (5.1) we will now relate the matrix L to the matrix K , by introducing index loop momenta b_m through $\vec{k} = \mathcal{O}\vec{b}$. We find the simple relation $K = L\mathcal{O}$, which allows to calculate λ ,

$$\lambda = \det(\mathcal{O})^2. \quad (5.2)$$

That is, the Schwinger parameters cancel.

Furthermore, we will show that $\det(\mathcal{O}) = 2$ holds for all graphs on RP^2 , whereas $\det(\mathcal{O}) = 1$ for all graphs on S^2 .

The problem of calculating \mathcal{O} factorizes into two sub-problems: An arbitrary graph on RP^2 looks like a planar graph with lines emerging from the boundary loop. These lines cross the boundary of the disk, enter the disk at the opposite boundary point and, finally, fuse the boundary loop again. So a graph actually separates into two parts: The boundary loop with the emerging lines and the interior of the planar graph. Suppressing the interior, the generic exterior part is shown in figure 1.

The two parts of the graphs can be treated separately. Of course, graphs on S^2 are treated implicitly, by suppressing the contribution of the exterior graph.

5.1 The interior graph

As just mentioned the interior graph looks exactly like a planar graph, with the outer loop omitted. Now in planar graphs the interior index momenta \vec{b} are exactly the loop momenta \vec{k} such that from

$$p_i = L_{ia}k_a = K_{im}b_m, \quad (5.3)$$

we see that $K = L$. The index i runs over propagators that do not cross the boundary of the disk, and the indices a and m label the loops and the index lines, which are actually the same.

We use the matrix \mathcal{O} introduced above for the basis change from the loop momenta k_a to the index momenta b_m ,

$$b_m = \mathcal{O}_{ma}^{-1}k_a. \quad (5.4)$$

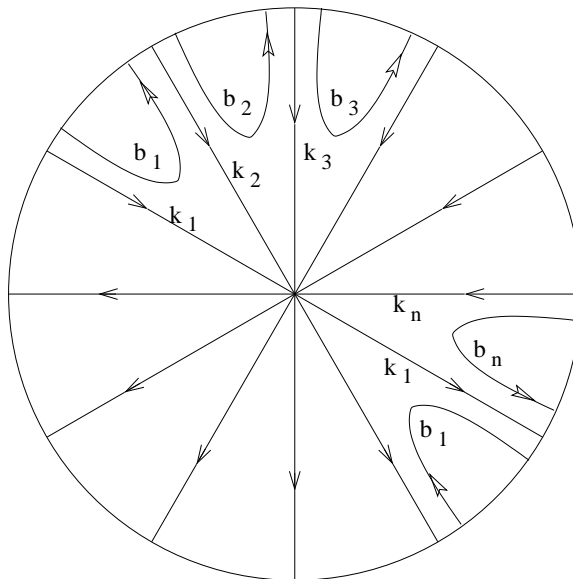


Figure 1: Star-diagram for generic graph on RP^2 . The labels b_i denote the momenta associated to the index loops. The loop momenta are denoted by k_a .

According to the factorization into interior and exterior graph \mathcal{O} splits as

$$\mathcal{O} = \begin{pmatrix} \mathcal{O}_{\text{int.}} & 0 \\ 0 & \mathcal{O}_{\text{ext.}} \end{pmatrix}. \quad (5.5)$$

For the interior momenta we just argued that the matrix $\mathcal{O}_{\text{int.}}$ obeys $\mathcal{O}_{\text{int.}} = \mathbf{1}$. Now we turn to the calculation of $\mathcal{O}_{\text{ext.}}$.

5.2 The exterior graph

By definition (4.2) the index loop momenta b_m are related to the propagator momenta p_i like

$$p_i = K_{im} b_m. \quad (5.6)$$

Here m, i run from 1 to n , the number of twisted propagators.³ The index loop momenta, on the other hand, give the loop momenta k_a . As can be read off from figure 1, the momenta flowing in the index lines b_i are related to the momenta in the canonical loops k_i like

$$\begin{aligned} k_1 &= b_1 + b_n, \\ k_l &= b_l - b_{l-1}, \quad l \neq 1. \end{aligned} \quad (5.7)$$

Thus we find the identity

$$K\mathcal{O}^{-1} = L. \quad (5.8)$$

Plugging this relation into the definitions of $M(s) = L^T S L$ and $N(s) = K^T S L$, we find, as promised

$$\lambda = \det(\mathcal{O})^2. \quad (5.9)$$

³Twisted propagators are propagators that cross the boundary of the disk.

It is easy to calculate the determinant of \mathcal{O} for arbitrary n . The value is

$$\det(\mathcal{O}) = 1 + (-1)^{n+1}(-1)^{n-1} = 2. \quad (5.10)$$

Hence, the value of the factor λ is

$$\lambda = \left(\frac{\det(N(s))}{\det(M(s))} \right)^2 = \det(\mathcal{O})^2 = 4. \quad (5.11)$$

6. Discussion of matrix model conjectures

After the cancellation of the fermionic and bosonic measures, the integrals over the Schwinger parameters (2.7) are given by

$$\int \prod_{i=1}^L ds_i e^{-s_i m} = \frac{1}{m^L}. \quad (6.1)$$

(L denotes the number of propagators, i.e. links in a given Feynman graph.) This factor can be reproduced by a mass term in the zero dimensional action $(m/2) \text{Tr}[\Phi^2]$. The combinatorial factors are reproduced by the Feynman rules of a zero dimensional field theory, i.e. a matrix model.

It was conjectured in [3] and later shown in [18, 17] that for the gauge group $U(N)$ the perturbative part of the effective superpotential $W_{\text{eff}}(S)$ can be obtained from a matrix model calculation as

$$W_{\text{eff}}^{\text{pert.}}(S) = N \frac{\partial \mathcal{F}_0(S)}{\partial S}, \quad (6.2)$$

where \mathcal{F}_0 is the planar contribution to the free energy of the $U(N)$ matrix model with potential equal to the tree level potential of the gauge theory. The S dependence of \mathcal{F}_0 is induced by identifying the 't Hooft coupling gN of the matrix model with the glueball-field S .

It was anticipated in [3] that for the gauge groups $SO(N)$ and $USp(N)$ one also has to take into account the contribution of the non-oriented matrix model diagrams. The above analysis suggests the form

$$W_{\text{eff}}^{\text{pert.}}(S) = N \frac{\partial \mathcal{F}_0(S)}{\partial S} + \lambda \mathcal{G}_0(S), \quad (6.3)$$

which differs from the conjecture [3] of the non-perturbative superpotential, as a factor N not $(N \mp 2)$ multiplies the derivative of $\mathcal{F}_0(S)$. Also we find a multiplicative factor in front of \mathcal{G}_0 , the RP^2 part of the matrix model free energy. The factor comes from the volume of the Schwinger moduli space (5.1), (5.2) and is given by $\lambda = 4$.⁴

Our explicit calculation of the next section indicates, that for a quartic tree level superpotential, (6.3) can be put into the form of (6.2) with the non-oriented part accounting for a shift $N \rightarrow N \mp 2$. We will comment on this case below.

⁴As already mentioned, the full effective superpotential also includes the Veneziano-Yankielowicz term $-(N \mp 2)[S \log(S/\Lambda^3) - S]$ [22], which in the matrix model is related to the volume of the gauge group [23].





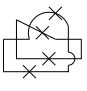

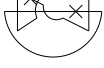






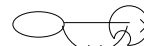
 2	  -4 1	$O(g^1)$
 2  2	 -8  -8  8	$O(g^2)$
 16  16	 -32  -32  -32  32	

Figure 2: Feynman graphs for perturbative calculation in $W_{\text{tree}}(\Phi) = (m/2) \text{Tr} \Phi^2 + 2g \text{Tr} \Phi^4$ up to two vertices.

7. Perturbative superpotential computations

In this section we explicitly calculate the effective superpotential for the gauge groups $SO(N)$ and $USp(N)$ with quartic tree level potential. We compare the contribution of non-orientable Feynman diagrams and planar ones. We will find a relation between the planar and the non-oriented contributions leading to a simplification of the matrix model description (6.3).

7.1 General prescription

With the results of the preceding sections at hand we can now rewrite the amplitudes in (4.9). We get

$$A_{\text{planar}}^\gamma = N h c_\gamma \left(\frac{1}{m} \right)^L S^{h-1} \quad (7.1)$$

for a given planar Feynman diagram γ . For the non-oriented diagrams we obtain

$$B_{RP^2}^\gamma = \sigma \lambda_{RP^2} c_\gamma \left(\frac{1}{m} \right)^L S^h. \quad (7.2)$$

We note that the powers of $16\pi^2$ in (4.7), (4.8), are canceled by $(4\pi)^{2l}$ coming from the bosonic momentum integration (3.4). (Remember that the number of loops l is related to the number of index loops h by $l = h - 1$ for the planar and $l = h$ for the non-oriented diagrams.)

7.2 Explicit calculations

We explicitly apply the rules from above to calculate the perturbative part of the superpotential for the tree level super-potential

$$W_{\text{tree}}(\Phi) = \frac{m}{2} \text{Tr } \Phi^2 + 2g \text{Tr } \Phi^4. \quad (7.3)$$

The combinatorial factors c_γ in equations (7.1), (7.2) receive contributions⁵ $(1/2)^L$ from the propagators (A.2), (A.8) and a factor of $2g$ from each vertex. The total is given by

$$c_\gamma = \left(\frac{1}{2}\right)^L (2g)^V \times (\text{combinatorics}). \quad (7.4)$$

The superpotential is then given by

$$W_{\text{eff}}^{\text{pert.}}(S) = N \left[3S^2 \left(\frac{g}{m^2}\right) + 36S^3 \left(\frac{g}{m^2}\right)^2 + \dots \right] + \sigma \lambda_{RP^2} \left[\frac{3}{2} S^2 \left(\frac{g}{m^2}\right) + \frac{36}{2} S^3 \left(\frac{g}{m^2}\right)^2 + \dots \right], \quad (7.5)$$

where $\sigma = \mp 1$ for the groups $\text{SO}(N)$ and $\text{USp}(N)$, respectively, and $\lambda_{RP^2} = 4$.

7.3 Discussion of example

The above result for $W_{\text{eff}}^{\text{pert.}}(S)$ is exactly of the form (6.2) with N shifted to $N \mp 2$ due to the non-oriented diagrams, where \mathcal{F}_0 is now the planar free energy of a $\text{SO}(N)/\text{USp}(N)$ matrix model with potential (7.3). Thus, up to order $O(S^4)$ we get

$$N \frac{\partial \mathcal{F}_0(S)}{\partial S} + \lambda \mathcal{G}_0(S) = (N \mp 2) \frac{\partial \mathcal{F}_0(S)}{\partial S}. \quad (7.6)$$

A factorization argument presented in [20] suggests that the relation (7.6) is exact. Consider $N = 2$ super Yang Mills, softly broken to $N = 1$ gauge theory by a quartic tree level potential. It was argued in [20] that the value at the minimum of the effective superpotentials for $\text{SO}(2KN - 2K + 2)$ (or $\text{USp}(2KN + 2K - 2)$) gauge groups is related to the value at the minimum of the effective superpotential of $\text{SO}(2N)$ (or $\text{USp}(2N)$) as

$$W_{\text{eff}}^{2KN \mp 2K \pm 2}(g, m) = K W_{\text{eff}}^{2N}(g, m), \quad (7.7)$$

for a fixed quartic potential $W_{\text{tree}}(\Phi) = m/2 \text{Tr } \Phi^2 + 2g \text{Tr } \Phi^4$. The value of the effective superpotential, calculated from the $N = 1$ approach and the $N = 2$ approach are related as shown in [21].

Applying the factorization (7.7) suggest for this example that

$$W_{\text{eff}}^{\text{pert.}}(S) = (N \mp 2) \frac{\partial \mathcal{F}_0(S)}{\partial S}. \quad (7.8)$$

⁵L, V and F will in the following denote the number of propagators, i.e. links, vertices and faces of a given Feynman graph. Furthermore we will use the relation $2V = L$ for the Φ^4 interaction.

$$1/2 \left(\begin{array}{c} \text{---} \text{---} \text{---} \text{---} \\ \text{k} \quad \quad \text{m} \\ \text{---} \text{---} \text{---} \text{---} \\ \text{l} \quad \quad \text{n} \end{array} - \begin{array}{c} \text{---} \text{---} \text{---} \text{---} \\ \text{k} \quad \quad \text{m} \\ \text{---} \text{---} \text{---} \text{---} \\ \text{l} \quad \quad \text{n} \end{array} \right)$$

Figure 3: The propagator of $SO(N)$ in double line notation.

$$\begin{array}{c} \text{---} \text{---} \text{---} \text{---} \\ \text{k} \quad \quad \text{m} \\ \text{---} \text{---} \text{---} \text{---} \\ \text{l} \quad \quad \text{n} \end{array} \quad \text{---} \quad \begin{array}{c} \text{---} \text{---} \text{---} \text{---} \\ \text{k} \quad \quad \text{m} \\ \text{---} \text{---} \text{---} \text{---} \\ \text{l} \quad \quad \text{n} \end{array}$$

Figure 4: The insertion of a commutator $[\mathcal{W}, \cdot]$ of $\mathcal{W} \in so(N)$ in double line notation.

Acknowledgments

We would like to thank O. Aharony, U. Fuchs, T. Sakai, J. Sonnenschein for valuable discussions. The research was supported by the US-Israel Binational Science Foundation. The research of H.I. is supported by the TMR European Research Network.

A. Double line notation

A.1 Double line notation for $SO(N)$

It is convenient to represent the Lie algebra of $SO(N)$ by antisymmetric $N \times N$ matrices M_{mn} , with the condition $M_{mn} = -M_{nm}$. In this notation adjoint fields are real antisymmetric $N \times N$ matrices

$$\Phi_{mn} = -\Phi_{nm}, \quad (\text{A.1})$$

and their free propagator in momentum space is proportional to the projector $P_{kl\ mn} = (1/2)(\delta_{km}\delta_{ln} - \delta_{lm}\delta_{kn})$,

$$\langle \Phi_{kl} \Phi_{mn} \rangle \sim \frac{1}{2}(\delta_{km}\delta_{ln} - \delta_{lm}\delta_{kn}). \quad (\text{A.2})$$

In double line notation we get figure 3.

The ends of the lines represent indices and the lines represent “deltas”.

Next we will consider insertions of the gauge fields

$$\exp(-s[\mathcal{W}^\alpha, \cdot]\pi_\alpha), \quad (\text{A.3})$$

in the double line notation. A simple commutator $[\mathcal{W}, \cdot]$ gives

$$\delta_{km}\mathcal{W}_{ln} - \mathcal{W}_{mk}\delta_{ln}. \quad (\text{A.4})$$

Pictorially the index contractions are drawn as in figures 4. If we use the property $\mathcal{W}_{km} = -\mathcal{W}_{mk}$ of the representation (A.1) $so(N)$, we can rewrite the commutator as

$$\delta_{km}\mathcal{W}_{ln} + \mathcal{W}_{km}\delta_{ln} \quad (\text{A.5})$$

and in double line notation the second term is denoted by figure 5 For the exponent (A.3) this generalizes to

$$\delta_{km} [\exp(-s\mathcal{W}\pi)]_{ln} + [\exp(-s\mathcal{W}\pi)]_{km} \delta_{ln}. \quad (\text{A.6})$$

The generalization of the above diagrams is straightforward.

$$\frac{\overline{k} \quad \overline{m}}{\overline{l} \quad \overline{n}} \overset{\text{W}}{\mid} \quad + \quad \frac{\overline{k} \quad \overline{m}}{\overline{l} \quad \overline{n}} \overset{\text{W}}{\mid} \quad \mid$$

Figure 5: The insertion of a commutator $[\mathcal{W}, \cdot]$ of $\mathcal{W} \in so(N)$ in double line notation, after applying the property $\mathcal{W}_{km} = -\mathcal{W}_{mk}$.

$$1/2 \left(\frac{\overline{k} \quad \overline{m}}{\overline{l} \quad \overline{n}} - \frac{\overline{k} \quad \overline{m}}{\overline{l} \quad \overline{n}} \right)$$

Figure 6: The propagator of an adjoint field of $USp(N)$ in double line notation.

$$\frac{\overline{k} \quad \overline{m}}{\overline{l} \quad \overline{n}} \overset{\text{W}}{\mid} \quad - \quad \frac{\overline{k} \quad \overline{m}}{\overline{l} \quad \overline{n}} \overset{\text{W}}{\mid} \quad \mid$$

Figure 7: The insertion of a commutator $[\mathcal{W}, \cdot]$ of $\mathcal{W} \in usp(N)$ in double line notation, after applying the property $M_{mn} = (JMJ)_{nm}$.

A.2 Double line notation for $USp(N)$

It is convenient to represent the Lie algebra of $USp(N)$, N even, by $N \times N$ matrices M_{mn} , with the condition $M_{mn} = (JMJ)_{nm}$, where J denotes the $USp(N)$ invariant skew symmetric form

$$J = \begin{pmatrix} 0 & \mathbf{1}_{N/2 \times N/2} \\ -\mathbf{1}_{N/2 \times N/2} & 0 \end{pmatrix}, \quad J^2 = -\mathbf{1}_{N \times N}. \quad (\text{A.7})$$

The propagator of a free adjoint scalar Φ_{mn} is proportional to the projector $P_{kl \ mn} = (1/2)(\delta_{km}\delta_{ln} - J_{lo}\delta_{om}J_{kp}\delta_{pn})$

$$\langle \Phi_{kl} \Phi_{mn} \rangle \sim \frac{1}{2}(\delta_{km}\delta_{ln} - J_{lm}J_{kn}). \quad (\text{A.8})$$

In double line notation J insertion are denoted by arrows, see figure 6. The orientation defined by the arrows is important, since J is antisymmetric and the order of its index contraction gives crucial (-1) factors. Insertions of a commutator can be rewritten using the properties $M_{mn} = (JMJ)_{nm}$ of $usp(N)$ to give

$$\delta_{km} \mathcal{W}_{ln} - (J\mathcal{W}J)_{km} \delta_{ln}. \quad (\text{A.9})$$

In double line notation these terms are shown in figure 7. Insertions of the gauge fields like in (A.3), factors⁶

$$\delta_{km} [\exp(-s\mathcal{W}\pi)]_{ln} + [J \exp(s\mathcal{W}\pi)J]_{km} \delta_{ln}. \quad (\text{A.10})$$

We used the properties of the $USp(N)$ generators to exchange the indices $k \leftrightarrow m$, and got two J s and a minus sign.

⁶Here we used the $\exp(J\mathcal{W}J) = -J \exp(-\mathcal{W})J$

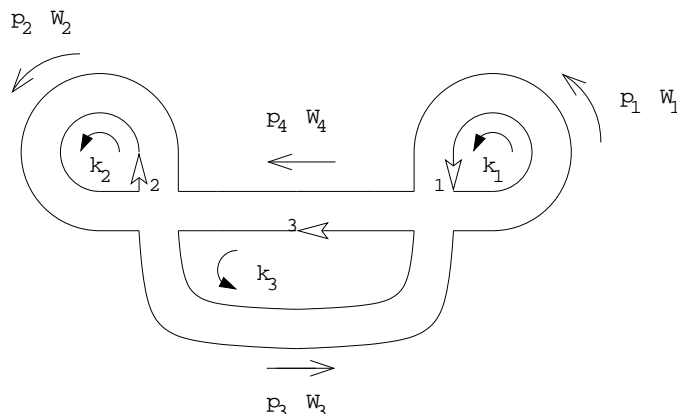


Figure 8: Planar Feynman diagram with loop momenta k_a , propagator momenta p_i , insertions W_i and three out of four index loops, indicated by empty arrows. The outer index loop is chosen to be free of insertions of W_i .

B. The matrices L_{ia} , K_{im}

In this appendix we will use explicit examples to illustrate the algorithm to determine the matrices L_{ia} and K_{im} .

B.1 Planar diagrams

The planar diagram we will analyze is given in figure 8. We denote the momenta associated to the propagators by p_i and the loop momenta by k_a . The W_i associated to the propagators are also written. The empty arrows indicate the index loops, where the subscript reminds us to associate the auxiliary variable \hat{W}_m to the respective index loop. As explained in the text for a planar diagram to be non-vanishing we have to choose one index loop to be free of insertions of the background field. This choice corresponds in figure 8 to the choice of putting the empty arrows on three out of the four index loops.

The matrix L_{ia} gives the expansion of the propagator momenta in terms of the loop momenta. For the graph in figure 8 we can make the following choice

$$p_1 = k_1, \quad p_2 = k_2, \quad p_3 = k_3. \quad (\text{B.1})$$

Furthermore momentum conservation at the vertices implies that $p_3 = p_4$ and thus $p_4 = k_3$. Hence, the matrix L_{ia} is given by

$$L = \begin{pmatrix} 1 & 0 & 0 \\ 0 & 1 & 0 \\ 0 & 0 & 1 \\ 0 & 0 & 1 \end{pmatrix} \quad (\text{B.2})$$

Some straightforward algebra then gives for the product $s_i(L^T)_{ai}L_{ib}$

$$\begin{pmatrix} s_1 & 0 & 0 \\ 0 & s_2 & 0 \\ 0 & 0 & s_3 + s_4 \end{pmatrix}. \quad (\text{B.3})$$

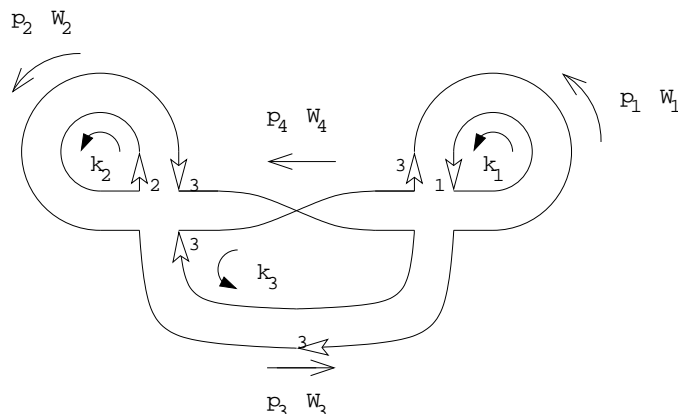


Figure 9: Non-orientable Feynman diagram with loop momenta k_a , propagator momenta p_i , insertions W_i and three index loops, indicated by empty arrows.

In order to obtain the matrix K_{im} we just need to read off from the diagram the contributions of each index loop to a given W_i taking into account the mutual orientation. This is done in the following way. Starting with W_1 we notice that there is only a contribution from the first index loop. Moreover, we have chosen the orientation of the index loop to be the same as the orientation of p_1 , such that we can write

$$W_1 = \hat{W}_1. \quad (\text{B.4})$$

A similar reasoning applies to the remaining W_i such that the matrix K relating the W_i to the auxiliary variables \hat{W}_m according to $W_i = K_{im} \hat{W}_m$ is given by

$$K = \begin{pmatrix} 1 & 0 & 0 \\ 0 & 1 & 0 \\ 0 & 0 & 1 \\ 0 & 0 & 1 \end{pmatrix}, \quad (\text{B.5})$$

which equals the matrix L as claimed in [18].

B.2 Non-oriented diagrams

B.2.1 The first non-oriented diagram

The first non-oriented diagram we will discuss is given in figure 9. The notation is the same as in the planar case. The only difference is that now due to the twist in one of the propagators the number of index loops is the same as the number of momentum loops and we do not have any free index loop.

The matrix L_{ia} is easily seen to be the same as in the planar diagram of figure 9. The matrix K_{im} on the other hand is modified. Applying the same strategy as in the planar case we find that now W_1 will receive contributions not only from index loop 1 but also from index loop 3. The orientation of index loop 1 is again chosen to be the same as the orientation of the momentum p_1 , whereas index loop 3 is oriented in the opposite way. The contribution from index loop 3 will therefore come with a negative sign and we can write

$$W_1 = \hat{W}_1 - \hat{W}_3. \quad (\text{B.6})$$

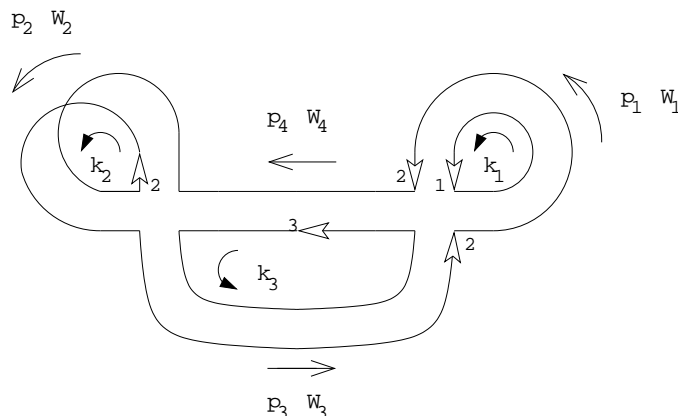


Figure 10: Non-orientable Feynman diagram with loop momenta k_a , propagator momenta p_i , insertions W_i and three index loops, indicated by empty arrows.

For \mathcal{W}_2 we obtain a similar result and for \mathcal{W}_3 , \mathcal{W}_4 we find that the third index loop contributes twice at a time with a negative sign leading to

$$\mathcal{W}_3 = -2\hat{\mathcal{W}}_3 = \mathcal{W}_4. \quad (\text{B.7})$$

Thus, the matrix K reads

$$K = \begin{pmatrix} 1 & 0 & -1 \\ 0 & 1 & -1 \\ 0 & 0 & -2 \\ 0 & 0 & -2 \end{pmatrix}, \quad (\text{B.8})$$

and the matrix $s_i(K^T)_{ni}L_{ib}$ is given by

$$\begin{pmatrix} s_1 & 0 & 0 \\ 0 & s_2 & 0 \\ -s_1 & -s_2 & -2(s_3 + s_4) \end{pmatrix}. \quad (\text{B.9})$$

B.2.2 The second non-oriented diagram

Our second non-oriented diagram is drawn in figure 10. The matrix K for this diagram is again obtained by applying the above algorithm. Reading off the contributions of the index loops we find

$$\begin{aligned} \mathcal{W}_1 &= \hat{\mathcal{W}}_1 + \hat{\mathcal{W}}_2, \\ \mathcal{W}_2 &= 2\hat{\mathcal{W}}_2, \\ \mathcal{W}_3 &= \hat{\mathcal{W}}_2 + \hat{\mathcal{W}}_3, \\ \mathcal{W}_4 &= \hat{\mathcal{W}}_2 + \hat{\mathcal{W}}_3, \end{aligned} \quad (\text{B.10})$$

leading to

$$K = \begin{pmatrix} 1 & 1 & 0 \\ 0 & 2 & 0 \\ 0 & 1 & 1 \\ 0 & 1 & 1 \end{pmatrix}. \quad (\text{B.11})$$

In this case the matrix $s_i(K^T)_{ni}L_{ib}$ is

$$\begin{pmatrix} s_1 & 0 & 0 \\ s_1 & 2s_2 & s_3 + s_4 \\ 0 & 0 & -(s_3 + s_4) \end{pmatrix}. \quad (\text{B.12})$$

References

- [1] R. Dijkgraaf and C. Vafa, *Matrix models, topological strings and supersymmetric gauge theories*, *Nucl. Phys. B* **644** (2002) 3 [[hep-th/0206255](#)].
- [2] R. Dijkgraaf and C. Vafa, *On geometry and matrix models*, *Nucl. Phys. B* **644** (2002) 21 [[hep-th/0207106](#)].
- [3] R. Dijkgraaf and C. Vafa, *A perturbative window into non-perturbative physics*, [hep-th/0208048](#).
- [4] N. Dorey, T.J. Hollowood, S. Prem Kumar and A. Sinkovics, *Exact superpotentials from matrix models*, *J. High Energy Phys.* **11** (2002) 039 [[hep-th/0209089](#)].
- [5] N. Dorey, T.J. Hollowood, S.P. Kumar and A. Sinkovics, *Massive vacua of $N=1$ * theory and S-duality from matrix models*, *J. High Energy Phys.* **11** (2002) 040 [[hep-th/0209099](#)].
- [6] F. Ferrari, *On exact superpotentials in confining vacua*, *Nucl. Phys. B* **648** (2003) 161 [[hep-th/0210135](#)].
- [7] H. Fuji and Y. Ookouchi, *Comments on effective superpotentials via matrix models*, *J. High Energy Phys.* **12** (2002) 067 [[hep-th/0210148](#)].
- [8] D. Berenstein, *Quantum moduli spaces from matrix models*, *Phys. Lett. B* **552** (2003) 255 [[hep-th/0210183](#)].
- [9] R. Argurio, V.L. Campos, G. Ferretti and R. Heise, *Exact superpotentials for theories with flavors via a matrix integral*, [hep-th/0210291](#).
- [10] J. McGreevy, *Adding flavor to Dijkgraaf-Vafa*, [hep-th/0211009](#).
- [11] I. Bena and R. Roiban, *Exact superpotentials in $N=1$ theories with flavor and their matrix model formulation*, [hep-th/0211075](#).
- [12] Y. Demasure and R.A. Janik, *Effective matter superpotentials from wishart random matrices*, *Phys. Lett. B* **553** (2003) 105 [[hep-th/0211082](#)].
- [13] S.G. Naculich, H.J. Schnitzer and N. Wyllard, *The $N=2$ $U(N)$ gauge theory prepotential and periods from a perturbative matrix model calculation*, [hep-th/0211123](#).
- [14] R. Dijkgraaf, S. Gukov, V.A. Kazakov and C. Vafa, *Perturbative analysis of gauged matrix models*, [hep-th/0210238](#).
- [15] R. Gopakumar, *$N=1$ theories and a geometric master field*, [hep-th/0211100](#).
- [16] A. Klemm, M. Marino and S. Theisen, *Gravitational corrections in supersymmetric gauge theory and matrix models*, [hep-th/0211216](#).
- [17] F. Cachazo, M.R. Douglas, N. Seiberg and E. Witten, *Chiral rings and anomalies in supersymmetric gauge theory*, *J. High Energy Phys.* **12** (2002) 071 [[hep-th/0211170](#)].
- [18] R. Dijkgraaf, M.T. Grisaru, C.S. Lam, C. Vafa and D. Zanon, *Perturbative computation of glueball superpotentials*, [hep-th/0211017](#).

- [19] S.J. Gates, M.T. Grisaru, M. Roček and W. Siegel, *Superspace, or one thousand and one lessons in supersymmetry*, *Front. Phys.* **58** (1983) 1 [[hep-th/0108200](#)].
- [20] H. Fuji and Y. Ookouchi, *Confining phase superpotentials for so/sp gauge theories via geometric transition*, [hep-th/0205301](#).
- [21] F. Cachazo and C. Vafa, *$N = 1$ and $N = 2$ geometry from fluxes*, [hep-th/0206017](#).
- [22] G. Veneziano and S. Yankielowicz, *An effective lagrangian for the pure $N = 1$ supersymmetric Yang-Mills theory*, *Phys. Lett.* **B 113** (1982) 231.
- [23] H. Ooguri and C. Vafa, *Worldsheet derivation of a large- N duality*, *Nucl. Phys.* **B 641** (2002) 3 [[hep-th/0205297](#)].